Convergence behaviour of Dirichlet–Neumann and Robin methods for a nonlinear transmission problem

Heiko Berninger*, Ralf Kornhuber, and Oliver Sander

Fachbereich Mathematik und Informatik, Freie Universität Berlin
berninger|kornhuber|sander@math.fu-berlin.de

Summary. We investigate Dirichlet–Neumann and Robin methods for a quasilinear elliptic transmission problem in which the nonlinearity changes discontinuously across two subdomains. In one space dimension we obtain convergence theorems by extending known results from the linear case. They hold both on the continuous and on the discrete level. From the proofs one can infer mesh-independence of the convergence rates for the Dirichlet–Neumann method, but not for the Robin method. In two space dimensions we consider numerical examples which demonstrate that the theoretical results might be extended to higher dimensions. Moreover, we investigate the asymptotic convergence behaviour for fine mesh sizes in these test cases quantitatively. We observe a good agreement with many known linear results, which is remarkable in view of the nonlinear character of the problem.

1 Introduction

The aim of this paper is to investigate the convergence behaviour of Dirichlet–Neumann and Robin methods for a quasilinear elliptic transmission problem and to compare it with well-known facts in the linear case. Theoretically, the linear convergence results in 1D can be carried over to the nonlinear case. Numerically, we find that the convergence behaviour in two nonlinear test cases is in good agreement with theoretical results in linear cases.

We consider the following setting. Let $\Omega \subset \mathbb{R}^n$ be a bounded Lipschitz domain divided into two non-overlapping subdomains Ω_1, Ω_2 with the interface $\Gamma = \overline{\Omega}_1 \cap \overline{\Omega}_2$, see Figure 1. The outer normal of Ω_1 is denoted by $\mathbf{n}$. Furthermore, let $f \in L^2(\Omega)$ and k_1, $k_2 \in L^\infty(\mathbb{R})$ with $k_i \geq \alpha > 0$ for $i = 1, 2$. In strong form the domain decomposition problem that we aim at reads:

Find a function p in Ω, $p_i := p_{|\Omega_i} \in H^1(\Omega_i)$, $i = 1, 2$, $p_{|\partial\Omega} = 0$, such that

* The work of this author was supported by the BMBF–Förderprogramm "Mathematik für Innovationen in Industrie und Dienstleistungen".

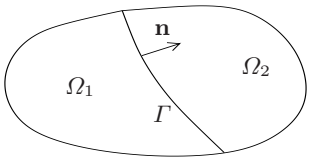

Fig. 1. Non-overlapping partition of the domain Ω

$$-\operatorname{div}(k_i(p_i)\nabla p_i) = f \qquad \text{on } \Omega_i,\ \ i = 1,2 \tag{1}$$
$$p_1 = p_2 \qquad \text{on } \Gamma \tag{2}$$
$$k_1(p_1)\nabla p_1 \cdot \mathbf{n} = k_2(p_2)\nabla p_2 \cdot \mathbf{n} \qquad \text{on } \Gamma\,. \tag{3}$$

For certain nonlinearities k_1 and k_2, this problem can be interpreted as a stationary nondegenerate Richards equation without gravity in a heterogeneous setting with two domains Ω_1 and Ω_2, that contain different soil types [4, Sec. 3.3.2].

A powerful tool to treat problems of this kind is to introduce new variables u_i, $i = 1, 2$, by Kirchhoff transformations κ_i (cf. [1]), defined by

$$u_i(x) := \kappa_i(p_i(x)) = \int_0^{p_i(x)} k_i(q)\,dq \quad \text{a.e. in } \Omega_i\,. \tag{4}$$

This entails $k_i(p_i)\nabla p_i = \nabla u_i$ and, therefore, problem (1)–(3) can be rewritten in the following form:

Find a function u in Ω, $u_{|\Omega_i} = u_i \in H^1(\Omega_i)$, $i = 1, 2$, $u_{|\partial\Omega} = 0$, such that

$$-\Delta u_i = f \qquad \text{on } \Omega_i,\ \ i = 1,2 \tag{5}$$
$$\kappa_1^{-1}(u_1) = \kappa_2^{-1}(u_2) \qquad \text{on } \Gamma \tag{6}$$
$$\nabla u_1 \cdot \mathbf{n} = \nabla u_2 \cdot \mathbf{n} \qquad \text{on } \Gamma\,. \tag{7}$$

As a consequence, in case of $k_1 \neq k_2$, we obtain a discontinuity of the primal variables and continuity of the dual variables across the interface, which is just converse in the original problem. Above all, though, the problems (5) on Ω_1 and Ω_2 are linear, and the nonlinearity of the problem is entirely contained in the interface equation (6). This consequence of the Kirchhoff transformation makes both the analysis and the numerical treatment of the transmission problem easier.

In the linear case, where k_i, $i = 1, 2$, are constant functions, Dirichlet–Neumann and Robin methods are well-understood iteration procedures for the treatment of non-overlapping elliptic domain decomposition problems, see, e.g., [12], [14] and [11]. We introduce nonlinear versions of these methods applied to (1)–(3) or (5)–(7), respectively, without using linearization. In one space dimension, both on the continuous and on the discrete level, we obtain convergence results by extending approaches used in the linear case, see [8] and [4]. We also obtain mesh-independent convergence rates for the

damped Dirichlet–Neumann method, but not for the Robin method, just as in the linear case. However, these generalizations of the convergence proofs for the linear setting do not work in dimensions higher than one. Therefore, we investigate the qualitative and quantitative convergence properties in 2D numerically.

Concerning the nonlinear Dirichlet–Neumann method, we observe asymptotically mesh-independent optimal convergence rates for a certain mesh-independent optimal damping parameter. Moreover, if the nonlinearities k_1 and k_2 are of different orders of magnitude, the Dirichlet–Neumann method converges considerably faster than if they are of the same order of magnitude. Strangely enough, this observation can be made plausible by investigations that have been carried out on corresponding settings for the Robin method in the linear case, see [10].

As to the nonlinear Robin method, we observe degenerating optimal convergence rates and parameters if the two Robin parameters involved in the method coincide. What is more, we can even establish formulas, which quantitatively describe the asymptotic behaviour of this degeneracy, and which are very similar to the ones, that have been discovered for the Robin method applied to the linear case, cf. [13]. Results from the theory of optimized Schwarz methods in linear cases (see, e.g., [11]) show, that the convergence speed can be further increased by allowing the two Robin parameters to be different. Indeed, we obtain a better asymptotic behaviour for our test cases if we choose the two parameters independently from each other. Finally, if the nonlinearities k_1 and k_2 are of different orders of magnitude, the optimized Robin method with different parameters converges quite fast with mesh-independent convergence rates, which, again, reproduces the situation in the linear case as considered in [10].

Altogether, the observations we made in our nonlinear numerical examples, resemble strikingly well the proved results for linear cases.

2 Transmission problem with jumping nonlinearities

In this section we introduce some further notation and give weak formulations of the problems (1)–(3) and (5)–(7). Furthermore, we point out the equivalence of these weak formulations with two versions of a Steklov–Poincaré interface equation.

In the following we use the notation and the definitions given in the introduction. In addition, cf. [14], we introduce (for $i = 1, 2$) the spaces

$$V_i := \{v_i \in H^1(\Omega_i) \,|\, v_{i|\partial\Omega\cap\partial\Omega_i} = 0\}, \quad V_i^0 := H_0^1(\Omega_i), \quad \Lambda := H_{00}^{1/2}(\Gamma)$$

and for $w_i, v_i \in V_i$ the forms

$$a_i(w_i, v_i) := (\nabla w_i, \nabla v_i)_{\Omega_i}\,, \qquad b_i(w_i, v_i) := (k(w_i)\nabla w_i, \nabla v_i)_{\Omega_i}\,,$$

where $(\cdot,\cdot)_{\Omega_i}$ stands for the L^2 inner product on Ω_i. The norm in Λ will be denoted by $\|\cdot\|_\Lambda$.

Let R_i, $i=1,2$, be any continuous extension operator from Λ to V_i. Then the variational formulation of problem (1)–(3) reads as follows:

Find $p_i \in V_i$, $i=1,2$, such that

$$b_i(p_i,v_i) = (f,v_i)_{\Omega_i} \qquad \forall v_i \in V_i^0,\ \ i=1,2 \tag{8}$$

$$p_{1|\Gamma} = p_{2|\Gamma} \qquad \text{in } \Lambda \tag{9}$$

$$b_1(p_1,R_1\mu) - (f,R_1\mu)_{\Omega_1} = -b_2(p_2,R_2\mu) + (f,R_2\mu)_{\Omega_2} \quad \forall \mu \in \Lambda\,. \tag{10}$$

Now, we understand the Kirchhoff transformations κ_i on $H^1(\Omega_i)$ in (4) as defined pointwise almost everywhere on Ω_i, $i=1,2$. Then problem (8)–(10) is transformed into:

Find $u_i \in V_i$, $i=1,2$, such that

$$a_i(u_i,v_i) = (f,v_i)_{\Omega_i} \qquad \forall v_i \in V_i^0,\ \ i=1,2 \tag{11}$$

$$\kappa_1^{-1}(u_{1|\Gamma}) = \kappa_2^{-1}(u_{2|\Gamma}) \qquad \text{in } \Lambda \tag{12}$$

$$a_1(u_1,R_1\mu) - (f,R_1\mu)_{\Omega_1} = -a_2(u_2,R_2\mu) + (f,R_2\mu)_{\Omega_2} \quad \forall \mu \in \Lambda\,. \tag{13}$$

For details concerning the Kirchhoff transformations in this sense, i.e., in the sense of superposition operators on $H^1(\Omega_i)$, see [5], where one can also find a proof of

Proposition 1. *Problems (8)–(10) and (11)–(13) are equivalent.*

Now, for a given $\lambda \in \Lambda$ (and omitting brackets for operators applied to λ from now on), we consider the harmonic extensions $H_i(\kappa_i\lambda) \in V_i$ of the Dirichlet boundary value $\kappa_i\lambda$ on Γ for $i=1,2$. With these operators and denoting by $\langle\cdot,\cdot\rangle$ the duality pairing between Λ' and Λ, we recall that the Steklov–Poincaré operators $S_i : \Lambda \to \Lambda'$ are defined by

$$\langle S_i\eta,\mu\rangle = a_i(H_i\eta,H_i\mu) \quad \forall \eta,\mu \in \Lambda\,, \quad i=1,2\,.$$

Furthermore, let $\mathcal{G}_i f$ be the solutions of the subproblems (11) with homogeneous Dirichlet data $(\mathcal{G}_i f)_{|\partial\Omega_i} = 0$. We define the functional $\chi = \chi_1 + \chi_2 \in \Lambda'$ by

$$\langle \chi_i,\mu\rangle = (f,H_i\mu)_{\Omega_i} - a_i(\mathcal{G}_i f,H_i\mu) \quad \forall \mu \in \Lambda\,, \quad i=1,2\,.$$

Now, it is easy to prove the following equivalence result, see [8].

Proposition 2. *By (4) and the relation*

$$u_i = H_i\kappa_i\lambda + \mathcal{G}_i f\,, \quad i=1,2\,,$$

between λ and u_i, the problems (8)–(10) and (11)–(13) are equivalent to the Steklov–Poincaré interface equation

$$\textit{find } \lambda \in \Lambda: \qquad (S_1\kappa_1 + S_2\kappa_2)\lambda = \chi \tag{14}$$

or, equivalently,

$$\textit{find } \lambda_2 \in \Lambda: \qquad (S_1\kappa_1\kappa_2^{-1} + S_2)\lambda_2 = \chi \tag{15}$$

if we set $\lambda_2 = \kappa_2\lambda$.

3 Nonlinear Dirichlet–Neumann and Robin methods

In this section we give a weak formulation of the nonlinear Dirichlet–Neumann and Robin methods that we apply to problem (11)–(13). We make clear what kind of iteration procedures these methods provide in terms of Steklov–Poincaré operators for the treatment of the interface equations. This will pave the way for proving the convergence of the methods in 1D by the application of Banach's fixed point theorem. All these considerations are closely connected to and can be infered from the linear theory, cf. [14] and [9]. We restrict ourselves to present the general line of thought and the main results. The proofs that we omit here can be found in [4] and will be published in detail and more general in further papers, see [6] and [7].

3.1 The methods and their Steklov–Poincaré formulations

We start with the nonlinear Dirichlet–Neumann method. Since its analysis and its numerical treatment is carried out in transformed variables, we present it for the domain decomposition problem (11)–(13). It reads as follows.

Given $\lambda_2^0 \in \Lambda$, find successively $u_1^{k+1} \in V_1$ and $u_2^{k+1} \in V_2$ for each $k \geq 0$ such that

$$a_1(u_1^{k+1}, v_1) = (f, v_1)_{\Omega_1} \qquad \forall v_1 \in V_1^0 \tag{16}$$

$$u_{1|\Gamma}^{k+1} = \kappa_1\kappa_2^{-1}(\lambda_2^k) \qquad \text{in } \Lambda \tag{17}$$

and then

$$a_2(u_2^{k+1}, v_2) = (f, v_2)_{\Omega_2} \qquad \forall v_2 \in V_2^0 \tag{18}$$

$$a_2(u_2^{k+1}, H_2\mu) - (f, H_2\mu)_{\Omega_2} = -a_1(u_1^{k+1}, H_1\mu) + (f, H_1\mu)_{\Omega_1} \quad \forall \mu \in \Lambda\,. \tag{19}$$

Then, with some damping parameter $\theta \in (0, 1)$, the new iterate is defined by

$$\lambda_2^{k+1} := \theta\, u_{2|\Gamma}^{k+1} + (1-\theta)\lambda_2^k\,. \tag{20}$$

This iteration procedure can be formulated equivalently for the original transmission problem (8)–(10). However, for the analysis (cf. [4, Sec. 3.3.2/3]), it is necessary to carry out the damping of the iterates in the transformed space. This is also reflected by the following link to the Steklov–Poincaré equation (15). Since a linear preconditioner seems to be necessary in this proposition, an analogous result for the symmetric equation (14), i.e., for untransformed variables, does not appear to be feasible.

Proposition 3. *The damped Dirichlet–Neumann algorithm (16)–(20) applied to (11)–(13) is a* preconditioned Richardson procedure *for the nonlinear Steklov–Poincaré equation (15) with S_2 as a preconditioner. Concretely, the iteration is given by the operator $T_\theta : \Lambda \to \Lambda$ defined by*

$$T_\theta : \lambda_2^k \mapsto \lambda_2^{k+1} = \lambda_2^k + \theta S_2^{-1}(\chi - (S_1\kappa_1\kappa_2^{-1} + S_2)\lambda_2^k)\,. \tag{21}$$

It is clear that we reobtain the situation for the linear case if we set $\kappa_1 = \kappa_2 = \mathrm{id}$. This also applies to the nonlinear Robin method to which we turn now. In contrast to the Dirichlet–Neumann method, the Robin iteration procedure is related to the symmetric Steklov–Poincaré equation (14), and it comes with two acceleration parameters $\gamma_1, \gamma_2 > 0$ rather than one. But just as the former, the latter method can be formulated equivalently for both problems (8)–(10) and (5)–(7). For the transformed problem (5)–(7) it reads:

Given a $u_2^0 \in V_2$ find successively $u_1^{k+1} \in V_1$ and $u_2^{k+2} \in V_2$ for $k \geq 0$ such that

$$a_1(u_1^{k+1}, v_1) = (f, v_1)_{\Omega_1} \quad \forall v_1 \in V_1^0 \tag{22}$$

$$\begin{aligned} a_1(u_1^{k+1}, R_1\mu) - (f, R_1\mu)_{\Omega_1} + \gamma_1(\kappa_1^{-1}u_1^{k+1}, \mu)_\Gamma = \\ - a_2(u_2^k, R_2\mu) + (f, R_2\mu)_{\Omega_2} + \gamma_1(\kappa_2^{-1}u_2^k, \mu)_\Gamma \quad \forall \mu \in \Lambda \end{aligned} \tag{23}$$

and then

$$a_2(u_2^{k+1}, v_2) = (f, v_2)_{\Omega_2} \quad \forall v_2 \in V_2^0 \tag{24}$$

$$\begin{aligned} a_2(u_2^{k+1}, R_2\mu) - (f, R_2\mu)_{\Omega_1} + \gamma_2(\kappa_2^{-1}u_2^{k+1}, \mu)_\Gamma = \\ - a_1(u_1^{k+1}, R_1\mu) + (f, R_1\mu)_{\Omega_1} + \gamma_2(\kappa_1^{-1}u_1^{k+1}, \mu)_\Gamma \quad \forall \mu \in \Lambda\,. \end{aligned} \tag{25}$$

As for the Dirichlet–Neumann method above, the following proposition provides a formulation of the Robin method in terms of Steklov–Poincaré operators for the solution of the corresponding Steklov–Poincaré equation. The result (cf. [4, Sec. 3.4.2]) generalizes linear theory in [9, Sec. 5.4]. We use the notation

$$\langle I\eta, \mu\rangle = (\eta, \mu)_\Gamma \quad \forall \eta, \mu \in \Lambda\,.$$

Proposition 4. *The Robin iteration procedure (22)–(25) applied to (11)–(13) is equivalent to the* Alternating Direction Iterative (ADI) method *applied to the Steklov–Poincaré equation (14). With a given $\lambda_2^0 \in \Lambda$ the ADI method means solving*

$$\begin{aligned} \langle(\gamma_1 I + S_1\kappa_1)\lambda_1^{k+1}, \mu\rangle &= \langle\chi + (\gamma_1 I - S_2\kappa_2)\lambda_2^k, \mu\rangle \qquad \forall \mu \in \Lambda \\ \langle(\gamma_2 I + S_2\kappa_2)\lambda_2^{k+1}, \mu\rangle &= \langle\chi + (\gamma_2 I - S_1\kappa_1)\lambda_1^{k+1}, \mu\rangle \quad \forall \mu \in \Lambda \end{aligned}$$

successively for $k \geq 0$. The equivalence to the Robin method is given in the sense of Proposition 2, i.e., by

$$u_i^k = H_i\kappa_i(\lambda_i^k) + \mathcal{G}_i f \iff \lambda_i^k = \kappa_i^{-1}(u_{i|\Gamma}^k) \quad \forall k \geq 0\,,\ \ i = 1, 2\,, \tag{26}$$

with the iterates u_i^k from (22)–(25). The operator

$$T_{\gamma_1,\gamma_2} : \Lambda \to \Lambda\,, \quad T_{\gamma_1,\gamma_2} : \lambda_2^k \mapsto \lambda_2^{k+1} \tag{27}$$

providing the ADI method and, equivalently, the Robin iteration, is given by

$$\lambda_2^{k+1} = (\gamma_2 I + S_2\kappa_2)^{-1}(\chi + (\gamma_2 I - S_1\kappa_1)(\gamma_1 I + S_1\kappa_1)^{-1}(\chi + (\gamma_1 I - S_2\kappa_2)\lambda_2^k))\,. \tag{28}$$

3.2 Convergence results

The approach for proving the convergence of the methods is based on considering the iteration operators T_θ in (21) and T_{γ_1,γ_2} defined in (27), (28), compare [4, Sec. 3.3/3.4]. First, it is not hard to see that a fixed point λ of the iterative scheme (21) or of the scheme given by (28) is a solution of the Steklov–Poincaré equation (15) or (14), respectively. Secondly, it is possible to extend theorems for the linear case and find conditions to be imposed on T_θ and T_{γ_1,γ_2}, respectively, so that Banach's fixed point theorem can be applied. This provides convergence of the iterative schemes as well as well-posedness of the domain decomposition problems.

The results look quite similar for the Dirichlet–Neumann and for the Robin method although the proofs are somewhat different. We give sufficient conditions guaranteeing convergence which are almost the same for both methods. However, for the Dirichlet–Neumann method they entail that $T_\theta : \Lambda \to \Lambda$ is a contraction if θ is small enough, whereas for the Robin method, only the composition of $T_{\gamma_1,\gamma_2} : \Lambda \to \Lambda$ with a continuous transformation of Λ can be proved to be a contraction, for equal but otherwise arbitrary γ_1 and γ_2. Since T_θ is a contraction, we obtain theoretical convergence rates in $[0, 1)$ for the Dirichlet–Neumann method on a continuous level, which turn out to be mesh-independent, i.e., they also apply to a discrete version of it. Since we do not know whether T_{γ_1,γ_2} is a contraction, this cannot be proved for the Robin method, and, even in linear cases, it is not true for the Robin iteration.

Again, we start with a convergence theorem for the Dirichlet–Neumann method, which is a generalization of a linear result to be found in [14, pp. 118/119].

Theorem 1. *Let β_2 and α_2 be the positive constants such that*

$$\langle S_2\eta, \mu\rangle \leq \beta_2\|\eta\|_\Lambda\|\mu\|_\Lambda \ \ \forall \eta, \mu \in \Lambda\,, \quad \langle S_2\eta, \eta\rangle \geq \alpha_2\|\eta\|_\Lambda^2 \ \ \forall \eta \in \Lambda$$

is satisfied, cf. [14, pp. 8/9]. Let $\kappa_1\kappa_2^{-1} : \Lambda \to \Lambda$ and, therefore, $S_1\kappa_1\kappa_2^{-1}$ be Lipschitz continuous, i.e., there is a constant $\beta_1 > 0$ such that

$$\langle S_1\kappa_1\kappa_2^{-1}\eta - S_1\kappa_1\kappa_2^{-1}\mu, \lambda\rangle \leq \beta_1\|\eta - \mu\|_\Lambda\|\lambda\|_\Lambda \quad \forall \eta, \mu, \lambda \in \Lambda\,. \tag{29}$$

Suppose there exists a constant $\kappa^* > 0$ *such that*

$$\langle S_1\kappa_1\kappa_2^{-1}\eta - S_1\kappa_1\kappa_2^{-1}\mu, \eta - \mu\rangle \geq \Big(\frac{\kappa^*}{2} - \alpha_2\Big)\|\eta - \mu\|_\Lambda^2 \quad \forall \eta, \mu \in \Lambda\,. \tag{30}$$

Then (15) has a unique solution $\lambda_2 \in \Lambda$*. Furthermore, for any given* $\lambda_2^0 \in \Lambda$ *and any* $\theta \in (0, \theta_{\max})$ *with*

$$\theta_{\max} := \frac{\kappa^*\alpha_2^2}{\beta_2(\beta_1 + \beta_2)^2}\,,$$

the sequence given by (21) converges in Λ *to* λ_2*. Theoretically optimal (i.e., minimal) convergence rates* ρ_{opt} *for corresponding optimal damping parameters* θ_{opt} *are given by*

$$\theta_{opt} = \frac{\theta_{\max}}{2} \qquad \textit{and} \qquad \rho_{opt} = 1 - \frac{\kappa^{*2}\alpha_2^2}{4\beta_2^2(\beta_1 + \beta_2)^2} = 1 - \frac{\kappa^*}{2\beta_2}\theta_{opt}\,. \tag{31}$$

The assumptions in Theorem 1 are satisfied in 1D.

Theorem 2. *In one space dimension,* $\kappa_1\kappa_2^{-1} : \Lambda \to \Lambda$ *is Lipschitz continuous, i.e., (29) holds, and* $S_1\kappa_1\kappa_2^{-1} : \Lambda \to \Lambda'$ *is a strongly monotone operator, i.e., (30) even holds with a* $\kappa^* > 2\alpha_2$*.*

We do not know if the assertion of Theorem 1 also holds in higher dimensions. However, there are counterexamples of operators $S_1\kappa_1\kappa_2^{-1} : \Lambda \to \Lambda'$ in 2D, that are not monotone, see [4, Sec. 3.3.4]. If Theorem 1 can be applied, it also has consequences for the untransformed problem (8)–(10) and for a discrete version of the transformed problem (11)–(13).

Theorem 3. *If the assumptions in Theorem 1 are satisfied, then problem (8)–(10) is well-posed. Moreover, we have* $p_i^k \to p_i$*,* $k \to \infty$*, in* V_i *for the iterates*

$$p_i^k = \kappa_i^{-1}(H_i\kappa_i\lambda^k + \mathcal{G}_i f) \in V_i\,, \quad i = 1, 2\,,$$

on Ω_i *which correspond via* $\lambda^k = \kappa_2^{-1}\lambda_2^k$*,* $k \geq 0$*, to the iterates* $(\lambda_2^k)_{k\geq 0}$ *of the Dirichlet–Neumann scheme (16)–(20).*

In addition, we assume that the problems in (11) and (13) are discretized by piecewise linear finite elements and that in (12) piecewise linear interpolation is applied to the function after having been Kirchhoff–transformed in the nodes of the interface. Then Theorem 1 can also be applied to this discretization with the same constants and, thus, leads to mesh-independent optimal convergence rates and optimal damping parameters.

For proving convergence of the Robin method (generalizing the linear result in [9, pp. 99/100]) we need $S_1\kappa_1, S_2\kappa_2 : \Lambda \to \Lambda'$ to be Lipschitz continuous and strongly monotone, which, by Theorem 2, is satisfied in 1D. Note that we do neither obtain convergence rates on the continuous level nor mesh-independence of optimal rates or parameters for the discretized problem.

Theorem 4. *Let $\gamma_1 = \gamma_2 = \gamma > 0$ and $\Omega \subset \mathbb{R}$ be one-dimensional. Then for any initial iterate $\lambda_2^0 \in \Lambda$ the operator $\mathcal{T}_\gamma = \mathcal{T}_{\gamma_1,\gamma_2}$ defined by (27), (28) provides a sequence $(\lambda_2^k)_{k\geq 0}$ which converges in Λ to the unique fixed point of $\mathcal{T}_\gamma$. Moreover, we have convergence of the sequences $(u_i^k)_{k\geq 1}$ and $(\kappa_i^{-1} u_i^k)_{k\geq 1}$ for $i = 1, 2$ given by (26) to the solutions of (11)–(13) and (8)–(10), respectively.*

For the discretization of problem (11)–(13) in Theorem 3 the corresponding discrete version of the Robin method converges to the discrete solution.

4 Parameter studies for the Dirichlet–Neumann method

The purpose of this section is to apply our nonlinear Dirichlet–Neumann method (16)–(20) on a discrete level to two concretely specified cases of the transmission problem in two space dimensions. In the next section we apply the nonlinear Robin method to the same test cases. Therefore, we first give a detailed description of these two examples here. After that, we present the numerical results that we obtained for the application of the Dirichlet–Neumann method. A discussion and an interpretation of the results as well as a comparison to the linear case follows.

We consider the transmission problem (1)–(3) on the unit Yin Yang domain Ω within a circle of radius 1 as shown in Figure 2 where one can see the coarse grid corresponding to level 1 of our calculations. We denote the white subdomain together with the grey circle B_1 by Ω_1 and the grey subdomain with the white circle B_2 by Ω_2. Furthermore, we select the data

$$f(x) = f_i \quad \text{on } B_i\,, \;\; i = 1, 2\,, \qquad f(x) = 0 \quad \text{elsewhere}\,,$$

and the nonlinearities

$$k_i(p_i) = \begin{cases} K_i\, p_{b,i} \max\{(-p_i)^{-3\lambda_i - 2},\, c\} & \text{for } p_i \leq -1 \\ 1 & \text{for } p_i \geq -1 \end{cases}$$

with certain parameters K_i, $p_{b,i}$, λ_i and a $c > 0$. These values are specified in Tables 1 and 2 for the two test cases that we want to consider.

Our choice represents a nondegenerate stationary Richards equation without gravity in a heterogeneous setting with two different soil types in Ω_1 and Ω_2 (see [15, Table 5.3.2]) and values f_1 and f_2 which can be regarded as a sink and a source, respectively. In Case I, which we call mildly heterogeneous, we only alter one soil parameter $\lambda_1 \neq \lambda_2$ when we go from one subdomain to the other. In the strongly heterogeneous case II, we change all parameters, in particular, the coefficients in front of the Laplacian have different orders of magnitude. In addition, with $c = 0.01$ the ellipticity constant, which enforces convergence, is more extreme in Case II than in Case I, where we choose $c = 0.1$.

Starting with the coarse grid (level 1) we successively carry out uniform refinement steps in order to obtain finer meshes, i.e., higher (refinement) levels.

Ω_i	f_i	λ_i	$p_{b,i}$	K_i
$i = 1$ (fine clay)	1.0	0.1	-1.0	$2.0 \cdot 10^{-3}$
$i = 2$ (coarse sand)	-1.0	1.0	-1.0	$2.0 \cdot 10^{-3}$

Table 1. Case I: mildly heterogeneous case

Ω_i	f_i	λ_i	$p_{b,i}$	K_i
$i = 1$ (clay)	$5.0 \cdot 10^{-5}$	0.165	-0.373	$1.67 \cdot 10^{-7}$
$i = 2$ (sand)	$-2.5 \cdot 10^{-3}$	0.694	-0.0726	$6.54 \cdot 10^{-5}$

Table 2. Case II: strongly heterogeneous case

For the discretization of (11)–(13) we use piecewise linear finite elements and apply the nonlinear transformation in (12) only in the nodes of the grid (as described in Theorem 3). Figures 3 and 4 show the solutions p on Ω for the mildly and the strongly heterogeneous case, respectively. They are calculated on level 6 with 235,000 nodes and have a range of $[-56.1, 0.9]$ in Ω_1 and $[-7.3, 5.7]$ in Ω_2 for Case I and $[-56.1, 0.0]$ in Ω_1 and $[-36.2, 3.0]$ in Ω_2 for Case II. The crater-like parts of the graphs (indicated by a black line in Figure 3) indicate the nonlinear (hydrologically, the unsaturated) regime of the equation.

For Case I, Figure 5 shows average convergence rates ρ of the Dirichlet–Neumann iteration with respect to the damping parameter θ on the first six levels, from the rightmost curve representing the first level to the leftmost curve corresponding to the 6th level. The convergence rates are given with respect to the transformed variables and are measured in the energy norms induced by the stiffness matrices on the relevant finite element spaces. Starting with the initial iterates $u_i^0 = 0$ for $i = 1, 2$, the Dirichlet–Neumann iteration is carried out until the relative error is below 10^{-12}. Each of the local problems on the subdomains is solved by 50 iterations of a linear multigrid which leads to numerically exact solutions. For the implementation we used the numerics environment DUNE, cf. [3], and the grid manager from UG, see [2].

In Figure 5 one can see that, as on the continuous level in Theorem 1, one obtains convergence if the damping parameter $\theta \in (0, 1)$ is below a threshold $\theta_{\max}$, and one observes optimal (i.e., minimal) convergence rates ρ_{opt} for a certain θ_{opt}. Both the threshold and the optimal parameter are level-dependent and decrease for higher levels. The corresponding optimal rates increase correspondingly. However, one also observes a stabilization of the optimal rates and the optimal damping parameters for higher levels. Concretely, the damping parameter $\theta_{opt} \approx 0.17$ leads to the optimal convergence rates $\rho_{opt} \approx 0.77$ on levels 5, 6 and 7 (see Figures 6 and 7). This indicates that mesh-independence is obtained in this two-dimensional case as was proved for

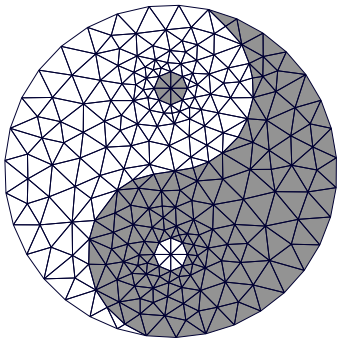

Fig. 2. Yin Yang domain Ω

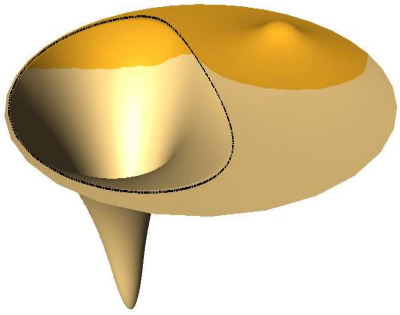

Fig. 3. Solution p on Ω in Case I (mildly heterogeneous)

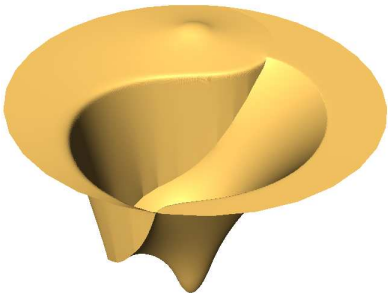

Fig. 4. Solution p on Ω in Case II (strongly heterogeneous)

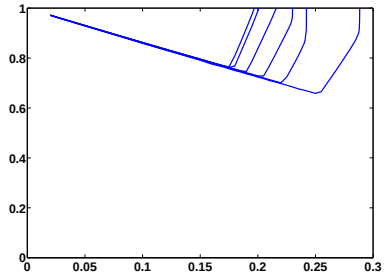

Fig. 5. ρ vs. θ on levels 1 (rightmost curve) to 6 (leftmost curve) in Case I

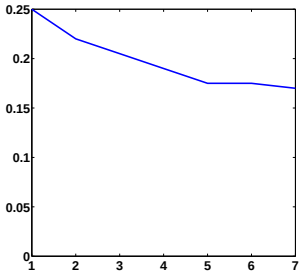

Fig. 6. θ_{opt} vs. level in Case I

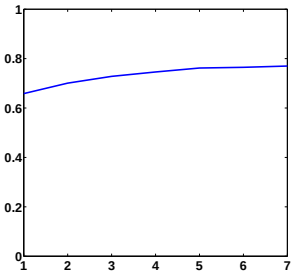

Fig. 7. ρ_{opt} vs. level in Case I

1D-cases (Theorem 3) and is known in linear settings (see [14, pp. 122–128] for additional quantitative results). Finally, we have the mesh-independent relationship $\rho_{opt} \approx 1 - \frac{7}{5}\theta_{opt}$ on all levels 1 to 7, which reflects (31).

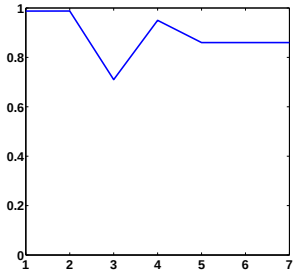

Fig. 8. θ_{opt} vs. level in Case II

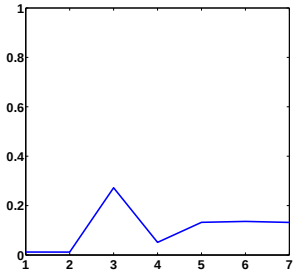

Fig. 9. ρ_{opt} vs. level in Case II

In principle, the situation for the strongly heterogeneous case II is the same as for Case I, see Figures 8 and 9. Again, optimal convergence rates corresponding to optimal damping parameters seem to stabilize asymptotically for high levels, but now we need considerably less damping $\theta_{opt} \approx 0.85$ for much better optimal rates $\rho_{opt} \approx 0.15$ (on levels 5, 6 and 7) than in Case I. In addition, even for overrelaxation, i.e., for parameters $\theta > 1$, convergence can be observed (concretely, we obtain $\theta_{opt} = \theta_{\max}/2$ as in (31)). In contrast to Case I, the convergence rates remain stable even if we choose a much smaller $c > 0$, e.g., $c = 10^{-100}$.

A possible reason for this considerably improved convergence behaviour of the Dirichlet–Neumann method might be the big jumps of the diffusion coefficients K_1 and K_2 in Case II, see Table 2. Surprisingly, the numerical results in the next section, where we present the convergence behaviour of the nonlinear Robin method for the two test cases, will shed some light on this phenomenon, again supported by linear theory. Here, we want to discuss this issue heuristically, regardless of the linear or nonlinear nature of the problem, by considering the corresponding constants in Theorem 1. Motivated by $K_1 \ll K_2$ in Table 2, we assume that $\alpha_2 \simeq \beta_2$ have the same order of magnitude which is "big" compared to $\alpha_1 \simeq \beta_1$ (where we assume $\kappa^*/2 - \alpha_2 =: \alpha_1 > 0$ in (30)). Then, considering (31), we estimate roughly

$$\rho_{opt} = 1 - \frac{\kappa^*}{2\beta_2}\theta_{opt} = 1 - \frac{\alpha_1 + \alpha_2}{\beta_2}\theta_{opt} \simeq 1 - \theta_{opt}$$

which, indeed, is the relation between θ_{opt} and ρ_{opt} on levels 1 to 7 in Figures 8 and 9. With the same arguments we find that

$$\theta_{opt} = \alpha_2 \frac{\alpha_1 + \alpha_2}{(\beta_1 + \beta_2)^2} \cdot \frac{\alpha_2}{\beta_2}$$

has the order of magnitude of α_2. Indeed, if we exchange the Dirichlet-subdomain Ω_1 and the Neumann-subdomain Ω_2, we only obtain convergence for very small damping parameters in Case II, whereas we do hardly see any

change in Case I. Also, the convergence rates are very bad for Case II after exchanging domains. This, however, cannot be inferred from the formula in (31), but by numerical stability: One can argue that the smaller K_1 is, the better the Dirichlet problem is conditioned on Ω_1 (with respect to the Dirichlet value), and the bigger K_2 is, the better the Neumann problem is conditioned on Ω_2 (with respect to the Neumann value). For more illuminating theory on linear cases with discontinuous coefficients, which confirms some of our findings in Case II, consult [10, p. 97]. Altogether, in such asymmetric cases, the asymmetry of the Dirichlet–Neumann method reveals itself dramatically.

5 Parameter studies for the Robin method

In this last section we present the numerical results that we obtained by applying the nonlinear Robin method (22)–(25) to the two test cases introduced in Section 4. In contrast to the Dirichlet–Neumann method, this leads to four different parameter studies. For both cases we first consider the Robin method with one Robin parameter $\gamma = \gamma_1 = \gamma_2$, for which our convergence result (Theorem 4) in 1D is valid, and secondly, we investigate the situation with different γ_1 and γ_2. Another difference between the Robin iteration and the Dirichlet–Neumann iteration is the nonlinear nature of each subproblem (22)–(23) and (24)–(25), for the solution of which we use a monotone multigrid method, see [4, Sec. 3.4.5]. The latter is stopped if the relative error of succeeding iterates in the energy norm drops below 10^{-12}. Otherwise, we use the same stopping criterion and average convergence rates as for the Dirichlet–Neumann method above.

Using the Robin iteration with $\gamma = \gamma_1 = \gamma_2$, we find that the numerical results of the two cases are virtually the same. Therefore, we only present Case II here. As one can see (on the logarithmic scale) in Figure 10, there are certain ranges for the Robin parameter γ on each level 1 to 6, where convergence rates are bounded away from 1. This is remarkable since Theorem 4 guarantees convergence for all $\gamma > 0$ in 1D. Furthermore—as for the Dirichlet–Neumann method—there is an optimal convergence rate ρ_{opt} obtained for an optimal γ_{opt} on each level. However—in contrast to the Dirichlet–Neumann method—these optimal rates and the corresponding parameters seem to degenerate rather than become asymptotically mesh-independent, compare Figures 12 and 13. The situation in Case I is almost the same as in Case II. However, the range of Robin parameters, for which an acceptable convergence speed is observed in the numerics, is about 10^4 times bigger than in Case II. Therefore, a good choice of γ seems to be correlated to the factor in front of the Laplacian (compare (23)), which is by some orders of magnitude bigger in Case I than in Case II.

In convergence proofs for the Robin method on the continuous level, as in the original [12], one usually does not derive convergence rates (compare

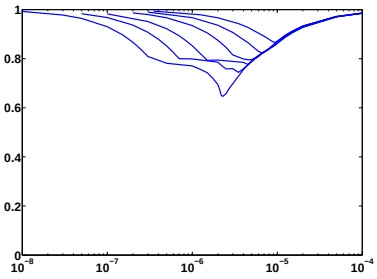

Fig. 10. ρ vs. γ on levels 1 (leftmost) to 6 (rightmost) for $\gamma_1 = \gamma_2$ in Case II

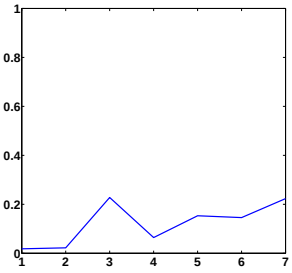

Fig. 11. ρ_{opt} vs. level for $\gamma_1 \neq \gamma_2$ in Case II

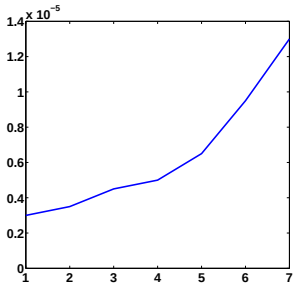

Fig. 12. γ_{opt} vs. level for $\gamma_1 = \gamma_2$ in Case II

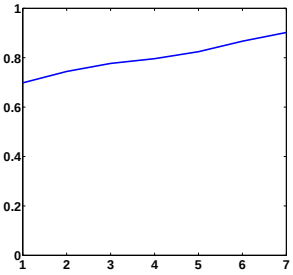

Fig. 13. ρ_{opt} vs. level for $\gamma_1 = \gamma_2$ in Case II

Section 3.2). This is because, usually, they are just not available. On the contrary, degeneracy of convergence rates is observed and proved on the discrete level for fine mesh sizes. In the world of optimized Schwarz methods the latter can even be formulated quantitatively as asymptotic convergence results. For example, in linear cases the asymptotic behaviour

$$\gamma_{opt}^{lin} = \mathcal{O}(h^{-1/2}) \quad \text{and} \quad \rho_{opt}^{lin} = 1 - \mathcal{O}(h^{1/2}) \tag{32}$$

of the optimal parameters and convergence rates with respect to the mesh size h is known for quite general domains, see [13]. Now, if we investigate the asymptotics in the nonlinear case II, displayed in Figures 12 and 13 with respect to h, we find

$$\gamma_{opt} = \mathcal{O}(h^{-0.45}) \quad \text{and} \quad \rho_{opt} = 1 - \mathcal{O}(h^{0.44})\,, \tag{33}$$

i.e., we do not only observe an asymptotic behaviour of a similar kind as in the linear case, but even with similar exponents. The situation for Case I is virtually the same.

The convergence speed of the Robin method can be further increased by allowing the Robin parameters γ_1 and γ_2 to be different. We have carried out

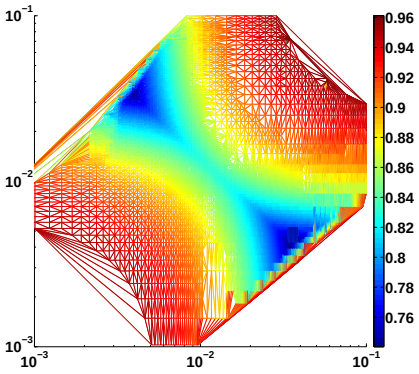

Fig. 14. ρ (colour) vs. γ_1 and γ_2 (x- and y-axes) on level 4 for Case I

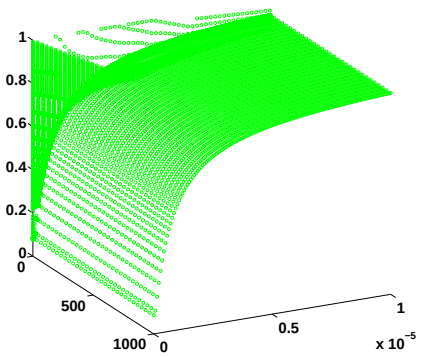

Fig. 15. ρ (height) vs. γ_1 and γ_2 (x- and y-axes) on level 4 for Case II

extensive numerical parameter studies for the performance of the nonlinear Robin method in both our cases on levels 1 to 8. Figures 14 and 15 shall serve as examples of the results we obtained on the 4th level in Case I (34,000 parameter pairs in a colour plot) and in Case II (77,000 parameter pairs in a height plot), respectively. First of all, in both graphics, which contain the case $\gamma = \gamma_1 = \gamma_2$ on the diagonal, one can clearly see that the convergence speed can be increased by an appropriate choice of different Robin parameters.

Now, however, the situations in Case I and in Case II are completely different. We start with considering Case I, where the slopes of the nonlinearities in the subdomains are different but not their order of magnitude. Here, we observe that the convergence rates are nearly symmetric with respect to the diagonal $\gamma_1 = \gamma_2$ and that two local minima occur off the diagonal—a left (global) one and a right one in Figure 14, which provide almost the same convergence rate,and for both of which $\gamma_{1,opt}$ and $\gamma_{2,\mathrm{opt}}$ are different. Although the convergence speed can be increased by choosing different instead of equal Robin parameters, asymptotically we still obtain degenerating optimal parameters and rates. However, we observe a weaker mesh-dependence of the convergence rates than for $\gamma_1 = \gamma_2$ in (33). Concretely, we find the asymptotic behaviour

$$\gamma_{1,opt} = \mathcal{O}(h^{-0.45}), \quad \gamma_{2,opt} = \mathcal{O}(h^{-0.41}) \quad \text{and} \quad \rho_{opt} = 1 - \mathcal{O}(h^{0.39}) \tag{34}$$

for the right minima and

$$\gamma_{1,opt} = \mathcal{O}(h^{-0.37}), \quad \gamma_{2,opt} = \mathcal{O}(h^{-0.55}) \quad \text{and} \quad \rho_{opt} = 1 - \mathcal{O}(h^{0.34}) \tag{35}$$

for the left (asymptotically global) minima.

As before in (32), our observations (34), (35) in the nonlinear case I can be compared to known results from the linear theory of optimized Schwarz

methods. In [11, p. 17] the asymptotic behaviour of different optimized Robin parameters and corresponding convergence rates has been derived for a linear equation on $\mathbb{R}^2$ decomposed into two half planes. The asymptotics is given by the formulas

$$\gamma_{1,opt}^{lin} = \mathcal{O}(h^{-1/4}), \quad \gamma_{2,opt}^{lin} = \mathcal{O}(h^{-1/4}) \quad \text{and} \quad \rho_{opt}^{lin} = 1 - \mathcal{O}(h^{1/4}). \tag{36}$$

A comparison with (36) shows that quantitatively the asymptotic behaviour of the different optimal Robin parameters in (34) and (35) does not seem to follow the linear results. Also, we do not obtain the same degree of acceleration of the convergence speed in (34) and (35) as suggested by the linear case (36). However, we observe the same kind of asymptotic behaviour for ρ_{opt} and, at least, the asymptotics lies between the situations (32) and (36).

In contrast to Case I, the situation in Case II is very unsymmetric with respect to the diagonal $\gamma_1 = \gamma_2$, and we do no longer observe two distinct local minima of convergence rates. We rather have a whole "valley" of parameter pairs, where one parameter γ_2 is more or less fixed while the other γ_1 is free (as long as it is big enough), in which nearly constant globally minimal rates occur. And even for the global minimum in this strip of parameter pairs, which is not at all distinct, one observes $\gamma_{1,opt} \approx 10^4\, \gamma_{2,opt}$ on levels 1 to 8. Most importantly, however, these globally minimal rates in the strip are asymptotically stable, i.e., mesh-independent, which can be seen in Figure 11, where the value for the 7th level is the same as for the 8th level. Note that with extreme values $\gamma_{1,opt} \gg \gamma_{2,opt}$ subproblems (22)–(23) and (24)–(25) resemble Dirichlet and Neumann problems, respectively, i.e., the Robin method becomes an undamped Dirichlet–Neumann method. This observation is quite striking if we compare Figure 11 for the optimized Robin method with two different parameters with Figure 9, which shows the optimal convergence rates for the damped Dirichlet–Neumann method.

We close this section by mentioning a known result on the Robin method applied to a linear equation with discontinuous coefficients $K_1/K_2 < 1$ in $\mathbb{R}^2$, decomposed into two half planes, see [10, p. 84]. The asymptotic behaviour in this case is given by

$$\gamma_{1,opt}^{lin} = \mathcal{O}(1), \quad \gamma_{2,opt}^{lin} = \mathcal{O}(h^{-1}) \quad \text{and} \quad \rho_{opt}^{lin} = \frac{K_1}{K_2} - \mathcal{O}(h^{1/2}).$$

Although, again, we cannot confirm the asymptotic behaviour for the optimized Robin parameters in our Case II, this rare result of a mesh-independent convergence rate for the Robin method makes our findings in this and in the previous section on the good convergence of our optimized methods in Case II a bit more understandable.

As a summary of our numerical test cases, we can say that, by and large, the numerical results of these last two sections resemble quite well the known theoretical results in linear situations.

Acknowledgement. We thank J. Schreiber for his assistance in producing the parameter studies.

References

1. H.W. Alt and S. Luckhaus. Quasilinear elliptic–parabolic differential equations. *Math. Z.*, 183:311–341, 1983.
2. P. Bastian, K. Birken, K. Johannsen, S. Lang, N. Neuß, H. Rentz-Reichert, and C. Wieners. UG – A flexible software toolbox for solving partial differential equations. *Comput. Vis. Sci.*, 1(1):27–40, 1997.
3. P. Bastian, M. Blatt, A. Dedner, C. Engwer, R. Klöfkorn, R. Kornhuber, M. Ohlberger, and O. Sander. A generic grid interface for parallel and adaptive scientific computing. Part II: Implementation and tests in DUNE. *Computing*, 82(2-3):121–138, 2008.
4. H. Berninger. *Domain Decomposition Methods for Elliptic Problems with Jumping Nonlinearities and Application to the Richards Equation*. PhD thesis, 2007.
5. H. Berninger. Non-overlapping domain decomposition for the Richards equation via superposition operators. In *Dom. Decomp. Meth. in Sc. and Engin. XVIII*, volume 70 of *LNCSE*, pages 169–176. Springer, 2009.
6. H. Berninger. Analysis of the Dirichlet–Neumann method for nonlinear transmission problems. 2010. In preparation.
7. H. Berninger and M. Discacciati. Analysis of the Robin method for nonlinear transmission problems. 2010. In preparation.
8. H. Berninger, R. Kornhuber, and O. Sander. On nonlinear Dirichlet–Neumann algorithms for jumping nonlinearities. In *Dom. Decomp. Meth. in Sc. and Engin. XVI*, volume 55 of *LNCSE*, pages 483–490. Springer, 2007.
9. M. Discacciati. *Domain Decomposition Methods for the Coupling of Surface and Groundwater Flows*. PhD thesis, 2004.
10. O. Dubois. *Optimized Schwarz Methods for the Advection-Diffusion Equation and for Problems with Discontinuous Coefficients*. PhD thesis, 2007.
11. M.J. Gander. Optimized Schwarz methods. *SIAM J. Numer. Anal.*, 44(2):699–731, 2006.
12. P.L. Lions. On the Schwarz alternating method. III: A variant for nonoverlapping subdomains. In *Dom. Decomp. Meth. for Part. Diff. Eq., Proc. 3rd Int. Symp.*, pages 202–223. SIAM, 1990.
13. S.H. Lui. A Lions non-overlapping domain decomposition method for domains with an arbitrary interface. *IMA J. Numer. Anal.*, 29(2):332–349, 2009.
14. A. Quarteroni and A. Valli. *Domain Decomposition Methods for Partial Differential Equations*. Oxford Science Publications, 1999.
15. W.J. Rawls, L.R. Ahuja, D.L. Brakensiek, and A. Shirmohammadi. Infiltration and soil water movement. In D.R. Maidment, editor, *Handbook of Hydrology*, chapter 5. McGraw–Hill, 1993.